X-611-68-497

MICROWAVE AND HARD X-RAY BURSTS FROM SOLAR FLARES

STEPHEN S. HOLT
REUVEN RAMATY

DECEMBER 1968

GSFC — GODDARD SPACE FLIGHT CENTER —
GREENBELT, MARYLAND

X-611-68-497
Preprint

MICROWAVE AND HARD X-RAY BURSTS FROM SOLAR FLARES

Stephen S. Holt
and
Reuven Ramaty*

December 1968

Goddard Space Flight Center
Greenbelt, Maryland

*NAS-NRC Resident Research Associate.

MICROWAVE AND HARD X-RAY BURSTS FROM SOLAR FLARES

by

Stephen S. Holt and Reuven Ramaty

ABSTRACT

We have applied detailed theories of gyro-synchrotron emission and absorption in a magnetoactive plasma, x-ray production by the bremsstrahlung of non-thermal electrons on ambient hydrogen, and electron relaxation in a partially ionized and magnetized gas to the solar flare burst phenomenon. The hard x-ray and microwave bursts are shown to be consistent with a single source of non-thermal electrons, where both emissions arise from electrons with energies $< mc^2$. Furthermore, the experimental x-ray and microwave data allow us to deduce the properties of the electron distribution, and the values of the ambient magnetic field, the hydrogen density, and the size of the emitting region. The proposed model, although derived mostly from observations of the 7 July 1966 flare, is shown to be representative of this type of event.

MICROWAVE AND HARD X-RAY BURSTS FROM SOLAR FLARES

INTRODUCTION

The discovery of high-energy x-rays from solar flares (Peterson and Winckler, 1959) and the excellent correlation between these events and impulsive radio bursts at centimeter wavelength (Kundu, 1961) have initiated several attempts to consistently reconcile these two classes of solar flare radiation (Takakura and Kai, 1966; DeJager, 1967; Holt and Cline, 1968). These studies indicate that the microwave and x-ray bursts can best be understood in terms of gyrosynchrotron emission and bremsstrahlung, respectively, from suprathermal electrons accelerated in the solar flare.

Kundu (1961) pointed out the striking temporal correlation between impulsive microwave bursts and x-ray emission, and subsequent investigation has shown that even the detailed time behavior of the highest energy x-rays reproduces that of the highest frequency microwave emission (Anderson and Winckler, 1962; Cline, Holt and Hones, 1968). This excellent time correlation seems to imply that both types of emission are produced by electrons of the same energies trapped in the same region of the solar atmosphere. Attempts to reconcile the x-ray and microwave bursts in terms of radiation from the same electron source, however, have yielded an apparent contradiction: the number of electrons required to produce the x-rays generally produces three to four orders of magnitude

more radio emission than is observed (Peterson and Winckler, 1959; Holt and Cline, 1968). Takakura and Kai (1966) have attempted to explain this discrepancy in terms of a model in which a major part of the x-ray producing electrons are invisible at radio frequencies by being trapped in a region below the plasma level corresponding to the highest observed microwave frequency. In this model, however, the microwave and x-ray bursts are produced by essentially two distinct electron sources, so that the temporal characteristics of the two emissions would not be expected to be as close as has been observed. Furthermore, for an optically thin radio source the observed spectral shape of the radio emission cannot be reproduced for any choice of magnetic field.

As pointed out in some of the studies of microwave and x-ray production in solar flares (e.g. Holt and Cline, 1968), the difficulty in reconciling these radiations in terms of a single electron source stems from the rather simplified treatments of the radiation mechanisms responsible for the observed emissions. While the ambient solar atmosphere will hardly affect the production and propagation of x-rays, it may significantly modify both the generation and propagation of radio waves through a variety of processes. In considering these effects we shall first discuss the various possible propagation phenomena. In addition to the absorption below the plasma frequency that was suggested by Takakura and Kai (1966), radio waves may also be absorbed by the ambient thermal electrons in the chromosphere and corona due to the processes of gyro-resonance and free-free absorption, and by the high-energy electrons themselves in the process of

gyro-synchrotron self-absorption. Owing to the low energies of the thermal electrons, however, gyro-resonance absorption (Zheleznyakov, 1962; Kakinuma and Swarup, 1962) is effective only at the first three harmonics of the local gyro-frequency and becomes negligible at higher harmonics where the major part of the radio emission is probably produced. Similarly, the process of free-free absorption cannot account for the required three to four orders of magnitude suppression, since, for typical chromospheric and coronal densities and temperatures, the optical depth of the overlying atmosphere is of the order of, or less than, unity (DeJager, 1967). Gyro-synchrotron reabsorption, on the other hand, may contribute significantly to the suppression of the radio emission since, unlike gyro-resonance absorption by thermal electrons, this process is effective at all frequencies where gyro-synchrotron emission is significant. It is conceivable, then, that the microwave radio source at the sun might by optically thick to its own radiation. The general theory of gyro-synchrotron reabsorption has been treated by several authors (Twiss, 1958; Kawabata, 1964; Kai, 1965b), but to our knowledge its importance for impulsive microwave bursts has not been investigated in the published literature.

With regard to generation effects, we first consider the influence of the ambient ionized medium on the production of gyro-synchrotron radiation; the ambient plasma reduces the emissivity of individual electrons at low frequencies. This phenomenon is commonly referred to as the Razin effect and its influence

on the spectral dependence of Type IV bursts at meter wavelengths was first investigated by Ramaty and Lingenfelter (1967). These authors showed that the observed low frequency cutoffs characteristic of Type IV bursts could result from the suppression of synchrotron emission owing to the influence of the ionized medium. Subsequently, Boischot and Clavelier (1967) reported an event which clearly exhibited such a low frequency cutoff and in a detailed analysis, based on a theoretical treatment of the influence of the ionized medium on gyrosynchrotron emission (Ramaty, 1968), Ramaty and Lingenfelter (1968) showed that the spectrum observed by Boischot and Clavelier (1967) can, indeed, be interpreted as a manifestation of the Razin effect. The importance of this effect for microwave bursts, however, has not yet been investigated in detail, even though much of the required suppression of the radio emission could result from the influence of the ionized medium. It should be pointed out, however, that when the radio source is optically thick to its own radiation, the Razin effect and reabsorption must be treated in a consistent fashion since these two processes are highly interdependent. As the influence of the medium becomes more pronounced, the Razin effect not only suppresses the emissivity of individual electrons but also reduces the corresponding absorption coefficient.

Finally, if the pitch-angle distribution of the radiating electrons at the sun is highly anisotropic the emitted radio power depends critically on the direction of observation with respect to the ambient magnetic field in the emitting region. Since this effect is significant for ultra relativistic electrons, but negligible for

lower energy particles, the observed emission at high frequencies in directions other than that of maximum anisotropy is much smaller than the radiation which would result from an isotropic electron distribution. At high frequencies, therefore, an anisotropic pitch-angle distribution may also contribute to the required suppression of the observed radio emission.

In order to take into account the various propagation and generation effects mentioned above, in the present paper we present the outline and the results of a more complete theory of microwave emission based on a detailed treatment of gyro-synchrotron emission and absorption by an arbitrary electron distribution in a magnetoactive plasma (Ramaty, 1969). In particular, we shall provide a consistent treatment of the Razin effect and gyro-synchrotron reabsorption, we shall consider the polarization of the radiation and we shall investigate the effects of an anisotropic electron distribution.

As mentioned above, the most likely radiation mechanism for high-energy x-ray production at the sun is bremsstrahlung of non-thermal electrons. A detailed discussion of bremsstrahlung cross sections and x-ray production by suprathermal electrons was given by Holt and Cline (1968). In the present paper we shall use these results to determine the expected x-ray fluxes at the earth from a given electron distribution at the sun.

For a complete understanding of the observed fluxes and time profiles of the microwave and x-ray bursts, however, we must also consider the expected

relaxation of the radiating electrons in the emitting region. This problem has been considered by Takakura and Kai (1966). In the present paper we present a similar treatment, which is more appropriate for the parameters that characterize our model of the microwave and x-ray emitting region, and which takes into account the various losses suffered by energetic electrons in a magnetized and partially ionized gas.

Using these theories of microwave production and absorption, x-ray production and electron relaxation in the flare region, we shall consider in detail the great flare of 7 July 1966. We shall show that it is possible to construct a consistent model in which both the x-rays and radio emission are produced by the same electron source in the same region of the solar atmosphere, where the ambient density is typical of the high chromosphere or low corona and is lower by about two to three orders of magnitude than the value obtained by Takakura and Kai (1966) for the x-ray emitting region. We shall also show that, at least for the flare of 7 July 1966, the required suppression of radio emission at the longer wavelengths is mainly the result of gyro-synchrotron reabsorption (and not the Razin effect), whereas at higher frequencies the emission is reduced either by a high-energy cutoff in the spectrum of the radiating electrons or by a strong anisotropy in their pitch-angle distribution. In addition, we shall show that the transition from frequencies where the source is optically thick to frequencies where it becomes optically thin leads to the change of the sense of

circular polarization which is consistent with the reversal of polarization that was observed for the 7 July 1966 flare as well as for numerous other microwave bursts.

From the observed microwave and x-ray fluxes for the flare of 7 July 1966 we can also estimate the total number of accelerated electrons at the sun. A comparison with direct electron measurements at the earth and quasi-thermal x-ray emission following the burst, allows us to investigate the problem of particle release from the flare region. Finally, the inferred optical depth allows us to estimate the angular size of the radio source and compare it with direct interferometric measurements (Kundu, 1965), thereby testing our contention that microwave bursts are optically thick due to reabsorption by the radiating electrons themselves.

X-RAY PRODUCTION

The x-radiation from solar flares is, basically, a manifestation of electron-proton bremsstrahlung. In the few-keV region, the emission is characteristic of a hot, optically thin source with strong emission lines and recombination edges superimposed on the free-free continuum. (Elwert, 1961). Above 10 keV, where the effect of line emission on the x-ray spectrum disappears, the observed spectra and decay characteristics are, again, consistent with a thermal continuum (Hudson, Peterson and Schwartz, 1969). As photon energies of ~ 100 keV are approached, however, both the shape of the spectrum and its decay characteristics

indicate a different source mechanism. The basic process is still electron-proton bremsstrahlung, but the source can no longer be consistently reconciled with the quasi-equilibrium thermal behavior of the lower energy x-rays (Holt and Cline, 1968).

The source function for the production of bremsstrahlung x-rays of reduced energy

$$\rho = \frac{h\nu}{mc^2} \tag{1}$$

may be written as

$$Q(\rho)\, d\rho = \int_{\rho}^{\infty} d\sigma(\gamma, \rho)\, n V J(\gamma)\, d\gamma \ \text{sec}^{-1} \tag{2}$$

where $J(\gamma)\, d\gamma$ is the differential electron flux (as a function of the electron Lorentz factor γ), n is the hydrogen density in the volume V, and $d\sigma$ is the appropriate cross section. As discussed by Holt and Cline (1968), a good approximation to this cross section at all energies is of the form:

$$d\sigma(\gamma, \rho) = \frac{4\alpha r_0^2 \gamma^2 d\rho}{\rho\{(\gamma^2 - 1)\,[(\gamma - \rho)^2 - 1]\}^{1/2}} \left[\left(\frac{\gamma - \rho}{\gamma}\right)^3 - \frac{2}{3}\left(\frac{\gamma - \rho}{\gamma}\right)^2 + \left(\frac{\gamma - \rho}{\gamma}\right)\right] .$$

$$\cdot \ln \left\{ \frac{(\gamma-\rho)\,(\gamma^2-1)^{1/2} + \gamma\,[(\gamma-\rho)^2-1]^{1/2}}{(\gamma-\rho)\,(\gamma^2-1)^{1/2} - \gamma\,[(\gamma-\rho)^2-1]^{1/2}} \right\} \cdot$$

$$\cdot \frac{1-\exp\{-2\pi\alpha\gamma(\gamma^2-1)^{-1/2}\}}{1-\exp\left\{-2\pi\alpha(\gamma-\rho)\,[(\gamma-\rho)^2-1]^{-1/2}\right\}} \tag{3}$$

where

$$\alpha = \frac{1}{137} \text{ and } r_0 = \frac{e^2}{mc^2} .$$

If the electron distribution is Maxwellian, one obtains the familiar result that, for unit Gaunt factor,

$$Q(\rho)\,d\rho \propto \frac{n^2 V}{\rho} \exp\left(-\frac{\rho}{kT}\right) \tag{4}$$

Below a few tens of keV, this characteristic thermal continuum and its decay via cooling are observed for all flares (Hudson, Peterson and Schwartz, 1969). If, on the other hand, a distinctly non-thermal electron spectrum is introduced, a quite different x-ray spectrum will be observed. For example, if we choose a form:

$$J(\gamma)\,d\gamma = A(\gamma-1)^{-\Gamma}\,d\gamma \tag{5}$$

for the electron flux, the source function will be (approximately):

$$Q(\rho)\, d\rho \propto Nn\, (\rho)^{-(\Gamma+1)} \tag{6}$$

where N is the total number of electrons above some lower energy limit in the volume. Nn, for the non-thermal source, plays the role of the quasi-thermal emission measure n^2V in normalizing the source function, except that Nn has an arbitrary value which depends upon the cutoff energy, while the measure n^2V takes into account all the electrons in the volume ($N/V \approx n$). We shall refer to Nn as an emission measure, and we wish to emphasize that, unlike the thermal emission measure n^2V, its numerical value depends upon the lower energy limit chosen, so that Nn will decrease as the non-thermal electron spectrum decays. For constant V, for example, Nn decreases while n^2V remains the same during the decay phase of the x-ray emission.

MICROWAVE PRODUCTION

We consider a homogeneous distribution of energetic electrons, characterized by a given energy spectrum and pitch angle distribution, moving in a homogeneous, collisionless and cold plasma permeated by a static and uniform magnetic field **B**. The emissivity $j(\nu, \theta)$ and absorption coefficient $K(\nu, \theta)$ for such a system of energetic electrons, in both the ordinary and extraordinary modes, can be derived from a general expression for the angular and frequency distribution of gyro-synchrotron radiation emitted by a single electron into a given mode of

wave propagation (Liemohn, 1965), and from an expression for the absorption coefficient appropriate for an anistropic electron distribution (Bekefi, 1966). If the distribution function in momentum space of the radiating electrons is separable into energy and pitch-angle dependent parts, $f(\gamma)$ and $g(\phi)$, respectively, the emissivity and absorption coefficient can be written as:

$$j_{\pm}(\nu,\theta) = \frac{BN}{V}\frac{\sqrt{3}e^3}{mc}\int_1^{\infty} d\gamma\, f(\gamma) \sum_{s=s_1}^{s_2} g(\phi_s)\,\eta_{\pm}\left(s, \frac{\nu}{\nu_B}, \gamma, \theta, \phi_s\right) \frac{\text{ergs}}{\text{cm}^3\,\text{sec}\,\text{sr}\,\text{Hz}} \tag{7}$$

$$K_{\pm}(\nu,\theta) = -\frac{N}{BV}(2\pi)^2\sqrt{3}e\frac{1}{n_{\pm}^2}\left(\frac{\nu_B}{\nu}\right)^2 \int_1^{\infty} d\gamma\, f(\gamma) \sum_{s=s_1}^{s_2} g(\phi_s)\,\eta_{\pm}\left(s, \frac{\nu}{\nu_B}, \gamma, \theta, \phi_s\right)$$

$$\cdot \left[\frac{\beta\gamma^2}{f(\gamma)}\frac{d}{d\gamma}\left(\frac{f(\gamma)}{\beta\gamma^2}\right) - \frac{n_{\pm}\cos\theta}{\beta\gamma\sin\phi_s}\left(1 - \frac{\cos\phi_s}{n_{\pm}\beta\cos\theta}\right)\frac{dg/d\phi}{g(\phi_s)}\right] \text{cm}^{-1} \tag{8}$$

where:

$$\eta_{\pm} = \frac{2\pi/\sqrt{3}}{\beta\gamma\cos\theta}\frac{s}{1 - n\beta\cos\theta\cos\phi_s}\frac{1}{1+\alpha_{\theta^{\pm}}^2}\left(1 + \frac{\partial \ln n_{\pm}}{\partial \ln \nu}\right)$$

$$\cdot \left[-\beta\sin\phi_s\, J_s'(x_s) + \left\{\alpha_{\theta^{\pm}}\left(\frac{\cot\theta}{n_{\pm}} - \beta\frac{\cos\phi_s}{\sin\theta}\right) + \frac{\alpha_{k^{\pm}}}{n_{\pm}}\right\} J_s(x_s)\right]^2 \tag{9}$$

and where

$$s_{1,2} = \frac{\nu}{\nu_B} \gamma (1 \pm n \ \beta \cos \theta) \tag{10}$$

$$x_s = \frac{s\, n_\pm \beta \sin \theta \sin \phi_s}{1 - n_\pm \beta \cos \theta \cos \phi_s} \tag{11}$$

$$\cos \phi_s = \frac{1 - s\, \nu_B / \gamma \nu}{n_\pm \beta \cos \theta} \tag{12}$$

The subscripts + or - indicate emission or absorption in the ordinary or extraordinary modes, respectively; β and γ are the velocity in units of c and the Lorentz factor of a radiating electron, respectively; N is the total number of the radiating electrons with energies greater than the arbitrarily chosen value of 100 keV; V is the total volume of the emitting region; ν_B is the cyclotron frequency of the ambient electrons; θ is the angle between the direction of observation and **B**; J_s is a Bessel function of order s; and $n_\pm (\nu, \theta)$ is the index of refraction of the ambient electron plasma and is, in general, frequency dependent and anistropic with respect to the direction of the magnetic field. The polarization coefficients $\alpha_{\theta\pm} (\nu, \theta)$ and $\alpha_{k\pm} (\nu, \theta)$ (Liemohn, 1965) are defined in terms of the components of the electric vector of the radiation field

$$i\,\alpha_\theta = \frac{E_\theta}{E_x}; \quad i\,\alpha_k = \frac{E_k}{E_x} \tag{13}$$

where E_x and E_θ are the transverse components of **E**, E_k is the component of **E** along the direction of propagation, and the x, θ and k axes are defined such that **B** lies in the (θ, k) plane.

For the purpose of the numerical evaluation of Equations (7) and (8), we shall assume that the radiating electrons have a low energy cutoff at 100 keV and that the distribution function $f(\gamma)\, g(\phi)$ is normalized to 1 electron per steradian with energies greater than 100 kev.

For a cold collisionless electron plasma the indices of refraction and polarization coefficients are given by (Ginzburg, 1964; Liemohn, 1965).

$$n_{\pm}^2 = 1 + \frac{2P^2 (P^2 - F^2)}{\pm [F^4 \sin^4\theta + 4F^2 (P^2 - F^2)^2 \cos^2\theta]^{1/2} - 2F^2 (P^2 - F^2) - F^2 \sin^2\theta} \tag{14}$$

$$a_{\theta\pm} = - \frac{2F (P^2 - F^2) \cos\theta}{- F^2 \sin^2\theta \pm [F^4 \sin^4\theta + 4F^2 (P^2 - F^2)^2 \cos^2\theta]^{1/2}} \tag{15}$$

$$a_{k\pm} = - \frac{P^2 F \sin\theta - a_{\theta\pm} P^2 \cos\theta \sin\theta}{P^2 (\cos^2\theta - F^2) - F^2 (1 - F^2)} \tag{16}$$

The dimensionless quantities F and P are defined in terms of the cyclotron and plasma frequencies

$$F = \nu/\nu_B; \quad P = \nu_P/\nu_B \tag{17}$$

where ν_B and ν_P are given in terms of the magnetic field B and the ambient electron density n_e by

$$\nu_B = \frac{1}{2\pi}\frac{eB}{mc}; \quad \nu_P = \frac{e}{\sqrt{\pi m}}\sqrt{n_e} \tag{18}$$

The indices of refraction, n_+ and n_-, have several cutoffs ($n = 0$) and resonances ($n \to \infty$). For $F > P$, or $\nu > \nu_p$, however, n_+ is real and less than 1, and for $F > \sqrt{P^2 + 1/4} + 1/2$, or $\nu > \sqrt{\nu_p^2 + \nu_B^2/4} + \nu_B/2$ n_- is also real and less than 1. It can be shown (Pawsey and Bracewell, 1955; Kundu, 1965) that, if one excludes propagation along the magnetic field, radiation at a frequency ν, in the ordinary or extraordinary modes, cannot escape from the solar atmosphere unless ν is greater than ν_p or $\sqrt{\nu_p^2 + \nu_B^2/4} + \nu_B/2$, respectively. We shall limit our discussion, therefore, to these frequency ranges only.

In previous studies of the effect of the ionized medium on solar radio emission (Ramaty and Lingenfelter 1967, 1968) it was convenient to introduce a parameter α, defined as

$$\alpha = \frac{3}{2}\frac{\nu_B}{\nu_p} = \frac{1.5}{P} \tag{19}$$

Then, in terms of this parameter, gyro-synchrotron emission from an electron of Lorentz factor γ is strongly suppressed at the low frequencies if $\alpha\gamma < 1$, but remains unaffected by the ionized ambient medium if $\alpha\gamma > 1$ (Ramaty, 1968). Moreover, if $\alpha\gamma \ll 1$, the total emission will also be strongly suppressed.

Since the index of refraction and polarization coefficients, as functions of ν/ν_B depend only on the "intrinsic" parameters α and θ, it is convenient to define two functions G and H, which are proportional to the emissivity and absorption coefficients respectively

$$G\left(\frac{\nu}{\nu_B}\right) = j \Big/ \frac{BN}{V}; \quad H\left(\frac{\nu}{\nu_B}\right) = K \Big/ \frac{N}{BV} \tag{20}$$

and which depend, therefore, only on α and θ and on the normalized distributions function $f(\gamma)\, g(\phi)$, but are independent of such "extrinsic" parameters as the intensity of the magnetic field, the site and shape of the radio source, and the densities of the energetic and ambient electrons.

Using Equations (7) through (20), we have evaluated numerically the functions $G(\nu/\nu_B)$ and $H(\nu/\nu_B)$ for a variety of values of the parameter α and θ and for several electron distributions $f(\gamma)g(\phi)$. As can be seen from Equations (13) and (16), the electric vector of the radiation field has a non-zero component, E_k, in the direction of propagation. Unless we invoke coupling between these longitudinal oscillations and transverse electromagnetic waves, the radiation associated with E_k will not escape from the sun. In computing the emission flux density at the earth, therefore, we have suppressed the longitudinal component of the radiation field by setting $\alpha_k = 0$. From the numerical calculations of $G(\nu/\nu_B)$, however, we find that for the frequency range mentioned above, the energy associated with E_k is negligible and, therefore, this approximate treatment of the boundary conditions at the sun does not seriously affect the calculated flux densities of the earth.

We now assume that the radio-source subtends a solid angle Ω at the earth, such that its volume is approximately given by

$$V \approx \Omega R^2 L$$

where R is the earth-sun distance and L is the depth of the radio source. The flux density at the earth is then given by

$$\phi_{\pm}(\nu, \theta) = \Omega \frac{j_{\pm}(\nu, \theta)}{K_{\pm}(\nu, \theta)} \left[1 - e^{-K_{\pm} L}\right] \frac{\text{ergs}}{\text{cm}^2 \,\text{sec}\, \text{Hz}} \qquad (21)$$

By defining an effective radiation area $A \approx \Omega R^2$, and by using Equation (20), Equation (21) can also be written as

$$\phi_{\pm}(\nu, \theta) = \frac{BN}{R^2} \frac{G_{\pm}(\nu/\nu_B)}{N/BA\, H_{\pm}(\nu/\nu_B)} \left[1 - e^{-\frac{N}{BA} H_{\pm}\left(\frac{\nu}{\nu_B}\right)}\right] \qquad (22)$$

As can be seen from this equation, the "extrinsic" properties of the source depend only on the parameters N/BA and BN. Apart from the dependence on the intrinsic parameters mentioned above, the importance of the reabsorption at a given frequency is determined only by N/BA. For electron energy spectra which decrease with increasing γ, $H(\nu/\nu_B)$ will be a decreasing function of frequency. For sufficiently large values of N/BA, therefore, at low frequencies the source will become optically thick to its own radiation and at these frequencies, for a given BN, the emission flux density will decrease with increasing N/BA. At higher frequencies the source will become optically thin and independent of N/BA, but the transition frequency from the optically thick to the optically thin regime will occur at higher frequencies for higher values of N/BA.

The emission flux density at low frequencies may be influenced not only by reabsorption (characterized by N/BA) but also by the Razin effect, the importance of which is determined by the parameter α. As discussed above, as α decreases, both the emissivity and absorption coefficient decrease and, therefore, for a given value of N/BA the radio source may be optically thick at low frequencies for a

large value of α but will become optically thin as α decreases. If for a given α the source is optically thick at low frequencies, the emission flux density will depend principally on the value of N/BA, whereas if for a given N/BA the source is optically thin, the emission depends mainly on the value of α.

From the numerical calculations mentioned above, we also find that as long as the emitting electrons are only mildly relativistic the emissivity in the extraordinary mode, j_-, is always greater than the emissivity in the ordinary mode, j_+. From these calculations we also find that the ratio j_+/K_+ is somewhat greater than j_-/K_- (by about 10% to 20%). This inequality is the result of the non-thermal character of the radiating electrons, since for a thermal electron distribution $j_+/K_+ = j_-/K_-$. An optically thin radio source, therefore, will always be polarized in a sense corresponding to the extraordinary mode. At frequencies for which the source becomes optically thick, however, the emission will be partially polarized in the ordinary mode and the sense of polarization will reverse at a frequency approximately equal to the transition frequency from the optically thick to the optically thin regime.

Finally, we wish to discuss the effects of variations of the angle of observation θ. For an isotropic pitch-angle distribution a variation in θ has the net effect of reducing the total emission and the emission frequencies, both approximately by a factor of sin θ. As long as θ is not equal to or very close to zero, these effects are small. On the other hand, however, for a highly anistropic

electron distribution, if θ differs significantly from the angle ϕ_m at which $g(\phi)$ is maximum, the emission from relativistic electrons is strongly suppressed. This effect is the direct result of the collimated synchrotron emission from ultrarelativistic electrons, and it becomes quite negligible for mildly relativistic particles.

In order to illustrate these effects and to compute the microwave flux densities at the earth, we have evaluated Equation (22) for $\theta = 45°$ and for various values of the parameters α and N/BA. In these computations we have used electron distributions of the form

$$f(\gamma)\, g(\phi) \sim (\gamma - 1)^{-\Gamma}\, e^{-\gamma/\gamma_0}\, \sin^m \phi\,. \tag{23}$$

As will be discussed below, from the x-ray observations of the July 7, 1966 flare, we find that $\Gamma \approx 3$. The parameter γ_0 defines a possible high-energy cutoff, which may result from escape or synchrotron losses of the high-energy electrons. Its value, however, must be greater than 2, since up to 500 kev at least, there is no evidence for such a cutoff in the observed x-ray data (Holt and Cline, 1968). Since the radio emission, however, is strongly influenced by a high-energy cutoff, we have considered the two limiting cases, $\gamma_0 = 2.5$ and $\gamma_0 \to \infty$. The parameter m determines the anisotropy of the electron distribution. We have again treated two extreme cases: $m = 0$, corresponding to an isotropic distribution, and $m = 45$ corresponding to a situation in which $g(80°)/g(90°) = 0.5$.

The results of these calculations are shown in Figures (1) and (2), for $\gamma_0 \to \infty$ and $\gamma_0 = 2.5$, respectively. As can be seen, the emission at high frequencies is strongly suppressed for the anistropic distribution. As mentioned above, this is the direct result of the collimated emission pattern of the high energy electrons and the large angle (45°) between the directions of observation and that of maximum anistropy.

The other dominant effect at high frequencies is the presence of a high-energy cutoff in the spectrum of the radiating electrons which introduces a corresponding high-frequency cutoff in the emission flux density. As can be seen from Figures (1) and (2), however, this cutoff is much less effective than that due to the anistropy and therefore the emission spectra from anistropic electron distributions become almost entirely insensitive to a high-energy cutoff in the electron spectrum.

At low frequencies, the emission spectra are dominated either by reabsorption of by the Razin effect. As can be seen from Figures (1) and (2) for large values of α (≥ 0.5), the emission spectra become independent of the Razin effect and are determined solely by the value of N /BA. For lower values of α the Razin effect becomes dominant, and, as can be seen for $\alpha = 0.35$, the emission spectra are almost independent of the value of N /BA.

The asterisks on the spectra in Figures (1) and (2) denote the frequencies ν^* at which the polarization changes from the ordinary to the extraordinary mode.

These frequencies are defined such that $\phi_+ (\nu^*) = \phi_- (\nu^*)$ and, as can be seen, they occur somewhat below the frequency at which the radio source becomes optically thin. For low values of α and low N /BA's ($\alpha = 0.35$ and N /BA = 10^{13} and 10^{14}) for which the source remains optically thin at all frequencies, the polarization does not change and the source is partially polarized in the extraordinary mode at all frequencies.

Finally, as can also be seen from Figures (1) and (2), the anistropy in the pitch-angle distribution has not only the effect of reducing the emissivity of the high-energy electrons, but also of shifting to lower values the frequency at which the change in polarization occurs. The dominance of the ordinary mode in a non-thermal optically thick source is caused by the greater relative contribution of the higher energy electrons to the emission in this mode of wave propagation. It is obvious, therefore, that an anistropic distribution which effectively reduces the emissivity from the higher-energy electrons will also reduce the range of frequencies at which the ordinary mode dominates.

ELECTRON RELAXATION

In attempting to deduce the time dependence of the x-ray and radio emission, we have assumed that a power law spectrum of electrons is accelerated in a time short compared to the decay time. The electrons then lose energy by virtue of their interaction with the ambient matter and the magnetic fields which pervade the medium.

The energy lost in x-ray producting bremsstrahlung is insignificant compared to that lost in radiationless collisions in the medium. Berger and Seltzer (1964) give the following expression for the power given up to neutral hydrogen by an electron of Lorentz factor γ:

$$-\frac{d\gamma}{dt}\Big|_{n\,coll} = 1.5\times10^{-14}\,\frac{n\gamma}{\sqrt{\gamma^2-1}}\cdot \left\{\ln\left[3.73\times10^{8}(\gamma^2-1)(\gamma+1)\right]+\frac{1}{\gamma^2}\left[1+\frac{(\gamma-1)^2}{8}-0.693(2\gamma-1)\right]\right\}\,sec^{-1} \tag{24}$$

For the source region, where we expect that most of the hydrogen is ionized, the power lost will increase owing to the ability of the medium to convert the electron kinetic energy to plasma modes. Using the results of Hayakawa and Kitao (1956), we can approximate the power lost in a medium of ionized fraction ϵ by the expression:

$$-\frac{d\gamma}{dt}\Big|_{\epsilon\,coll} \approx (2\epsilon+1)\left[-\frac{d\gamma}{dt}\Big|_{n\,coll}\right]\,sec^{-1}. \tag{25}$$

In the subsequent calculations, we shall take $\epsilon \approx 1$.

The other important contributor to the power lost by the electrons is gyro-synchrotron emission in the ambient magnetic field. This loss term may be written

$$-\frac{d\gamma}{dt}\Big|_{mag} = 1.9\times10^{-9}\,\beta^2\,\gamma^2\,B_\perp^2\,sec^{-1}. \tag{26}$$

The influence of the ionized medium on the emission through the parameter α, defined in Equation 19, decreases the emissivity of the electrons, but does not substantially affect the power lost (i.e. the decreased emissivity in electromagnetic radiation is compensated by energy transferred to plasma modes of the medium).

By comparing Equations (24) and (26), we see that the energy dependence of the collision term is exceedingly weak compared to that of the magnetic term. Furthermore, the energy dependences tend to be in opposite directions, such that the magnetic losses increase with increasing energy, while the collision losses decrease slightly with increasing energy. This means that we can, in principle, deduce which of these loss terms is the more important by observing the temporal dependence of the spectral shape (a steepening spectrum with time would imply a dominant magnetic loss term, while a relatively constant, or slightly hardening, spectrum would characterize collision loss).

In Figure (3) we have displayed the relaxation of a distribution of electrons with an initial spectrum of the form:

$$N(\gamma)\, d\gamma = A(\gamma - 1)^{-3}\, d\gamma \qquad (27)$$

As we shall see, below, this is a good representation of the actual case. The parameter α relates the magnetic field to the hydrogen density, so that the choice of the hydrogen density immediately determines all field values and times

indicated in the figure. The figure is constructed such that the electron density at 100 keV is the same for each value of α. Note that, as long as α is less than about 3, the temporal behavior below approximately mc^2 is virtually independent of α, indicating that the decay of the electron spectrum in this range is clearly collision-dominated. At higher energies, however, the effect of the magnetic field is reflected in the variation of spectral shape.

PHYSICAL CONDITIONS IN THE EMITTING VOLUME

The great flare of July 7, 1966 was the first instance in which the differential spectrum of x-rays up to $\sim$ 500 keV was measured (Cline, Holt and Hones, 1968). The spectral shape, and its constancy (or possible hardening) in time during the decay, imply a non-thermal, collision-dominated electron source for the x-ray emission. The x-ray data has been fit (Holt and Cline, 1968) with a power law in the electron flux. Since the radio emission calculations are density- rather than flux-dependent, we have refit the data to a power law in the electron density with no substantial reduction in the goodness of fit. This spectrum is displayed in Figure 4.

We have chosen to fit the data with the same spectral index in the density, -3, which Holt and Cline (1968) used for the flux. This means that the index is approximately half a power flatter than the actual best fit (as evidenced by Figure 4) but, as will be shown below, this is a more severe test of the adequacy of the model which we propose.

The non-thermal emission measure deduced from Figure 4 for the spectral index -3, for electrons with energy in excess of 100 keV at emission maximum, is

$$Nn \approx 4.1 \times 10^{45} \text{ cm}^{-3} \tag{28}$$

If the decay of the emission is dominated by collision losses, as the relative constancy of the x-ray spectrum throughout the decay would indicate, then, as can be seen from Figure 3 for electrons of a few hundred keV, the one-minute x-ray decay time implies a hydrogen density of about 2×10^9 cm^{-3}.

A striking feature of the x-ray source is exhibited in Figure 5, where the temporal behaviors of the > 80 keV x-ray emission and 17,000 MHz radio emission are compared. Note that all of the detailed features of the temporal behavior of the high-energy x-ray emission are reproduced in the high frequency radio history, indicating an intimate connection between the two emissions. This is the prime reason that we attempt to construct a model in which the microwave emission can be accounted for by the same electron source that produces the x-rays.

The observed peak microwave spectrum is shown in Figure 6 (Nagoya, 1966) together with radio spectra which were obtained from the calculations described in a previous section and which correspond to representative parameters described below. As can be seen, the observed radio spectrum is significantly flatter

than those calculated. It is our opinion, however, that such a flatter spectrum could be reproduced by considering a distribution of field strengths and ambient densities at the site of the emission, rather than treating the simple case of a unique and uniform field and a constant density. This averaging procedure, however, would introduce additional unknown parameters which would unnecessarily complicate the problem. As indicated in Figure 6, we have normalized the calculated and observed radio emissions in the central portion of the observed emission, at 3750 MHz, which we have arbitrarily assumed to correspond to a frequency 0.4 ν_m, where ν_m is the computed frequency of maximum emission.

Using this normalization, we have compared the calculated spectra for each choice of N/BA and α shown in Figures 1 and 2 with the observed flux density shown in Figure 6. From these comparisons we can deduce the magnetic field B and the product BN, which together with the emission measure Nn yield the target density, n, and the total number of electrons greater than 100 keV, N. Assuming that the ambient medium is a completely ionized hydrogen gas ($n_e = n$) we can compute the value of α corresponding to the deduced values of B and n. This procedure was carried out for all spectra shown in Figures 1 and 2 and the results for the isotropic distribution with a high-energy cutoff and for the anisotropic distribution are summarized in Tables 1 and 2, respectively. We do not show the calculations for the isotropic distribution with no high-energy cutoff, since in this case the calculated radio fluxes at the high frequencies are

much larger than the observed flux density and, therefore, they cannot be consistently reconciled with the x-ray observations. We also omitted the calculations for the anisotropic distribution with $\alpha = 0.35$, $N/BA = 10^{13}$ and 10^{14}, since, as can be seen from Figures 1 and 2, the computed spectra are much too steep to account for the observations. From Tables 1 and 2, we see that for each value of N/BA one can find a consistent value of α, which we have denoted by $\bar{\alpha}$. Furthermore, from Figures 1 and 2 it follows that these values of $\bar{\alpha}$ are such that the low frequency features of the radio source are determined by reabsorption and not by the Razin effect, so that the important parameter is N/BA and not α. The similarity of the observed microwave and x-ray spectra for the 7 July 1966 event with those from other large flares (e.g. 23 May 1967, 28 August 1967) would indicate that this result is a fairly general feature of microwave bursts from large solar flares.

The values of the ambient density, n, magnetic field, B, and total number of high energy electrons, N, for three choices of the parameter N/BA and the corresponding consistent value of α are shown in Table 3. Also shown in this Table are the deduced values of the effective radiation area, A, and a mean electron emission Lorentz factor, $\bar{\gamma}$, which is defined such that the integrand in Equation (7) is a maximum at $\gamma = \bar{\gamma}$. As can be seen, both the ambient density and magnetic field decrease for increasing N/BA and at the same time the total number of electrons and $\bar{\gamma}$ increase. Even though the values of n and B at the

site of emission are unknown, the ranges of the parameter N/BA can be determined from the requirement that the radio-emitting electron energies should be approximately the same as those responsible for the x-ray emission. Since the highest observed x-ray energy is ~ 500 kev, we shall demand that $\bar{\gamma} \leq 2$. Therefore, from Table 3, N/BA cannot be larger than 10^{13} in the case of an isotropic distribution with a high-energy cutoff, in which case the ambient density must be as high as 3×10^{10}. As was discussed above, however, the mean density in the emitting region cannot be greater than about 2×10^{9} cm^{-3} if the decay of the x-ray burst is the result of collision loss. A density as high as 3×10^{10} cm^{-3}, therefore, cannot be reconciled with the observations unless there is significant non-impulsive acceleration during the decay phase of the event. This possibility cannot be ruled out on the basis of the present calculations and the available data. On the other hand, as can be seen from Table 3, the radio emission of the high-energy electrons (for an anistropic distribution) is sufficiently suppressed so that ambient densities as low as 2×10^{9} cm^{-3} and mean electron energies around 400 keV could be consistent with both the peak x-ray and microwave fluxes. In this case, therefore, acceleration is not required during the decay phase of the burst, since the observed decay time is consistent with the collision losses the electrons would suffer in the ambient medium.

The calculated flux densities at the earth for the anisotropic distribution, for an ambient density of 3×10^{9} cm^{-3} and $N/BA = 10^{14}$ (consistent with essentially no acceleration during the decay phase of the event), and for the isotropic

distribution with a high-energy cutoff, for an ambient density of 3×10^{10} cm^{-3} and $N/BA = 10^{13}$ (which requires considerable re-acceleration), are shown in Figure 6. Also shown in this figure is the observed peak flux density for the 7 July 1966 event (Nagoya, 1966). The data point at 17000 MHz is a lower limit because of detector saturation, and therefore the observed spectrum could have peaked at frequencies greater than 9400 MHz, in which case the deduced values of B would become somewhat larger than the ones given in Table 3. As in Figures 1 and 2, the asterisks denote the frequencies at which the sense of polarization reverses. The values of these frequencies, corresponding to the two electron distributions we have used, bracket the observed frequency of polarization reversal of ~ 3750 MHz (Nagoya, 1966).

We now consider the values of the area A given in Table 3. If one restricts the possible range of parameters to values such that $\overline{\gamma} \lesssim 2$, then A is of the order of 5×10^{19} cm^2. This corresponds to an angular size of about 1.6 minutes of arc which is in good agreement with interferometric measurements of the angular size of microwave bursts (Kundu, 1965). This seems to lend further support to our contention that the microwave radio source at low frequencies is optically thick (the reabsorption being due to the high-energy electrons themselves), and that, therefore, the observed change in polarization is, indeed, due to the transition from the optically thick to the optically thin regime.

Finally, we wish to discuss the deduced values for the total number of electrons required to produce the x-ray and microwave emissions. For the acceptable range of values of $\bar{\gamma}$ shown in Table 3, the total number of flare accelerated electrons with energies greater than 100 keV ranges from about 2×10^{35} to 8×10^{36} electrons for the anistropic distribution, and it is not more than 1.4×10^{35} electrons for the isotropic case with a high-energy cutoff. From direct electron measurements at the earth, Cline and McDonald (1968) have deduced that for the flare of 7 July 1966 about 5×10^{31} electrons with energies greater than 3 MeV were released from the sun into interplanetary space.

Obviously, one cannot directly compare the observations at the earth at energies greater than 3 MeV with our estimates in the source region based on an electron spectrum with a high-energy cutoff at about 750 keV. Therefore, we shall first consider the anisotropic case for which no high-energy cutoff is necessary. Assuming that at the site of the emission the $(\gamma - 1)^{-3}$ spectrum extends up to the highest electron energies observed at the earth, the microwave and x-ray observations would require that about 2.2×10^{32} to 9×10^{33} electrons greater than 3 MeV be accelerated in the flare. Comparing these numbers with that deduced by Cline and McDonald (1968), we conclude that only about 0.6% to 23% of the relativistic electrons produced in the flare escaped from the sun. Ramaty and Lingenfelter (1968), who investigated a Type IV burst associated with the 14 September 1966 flare (Boischot and Clavelier, 1967) arrived at a

similar conclusion, namely that only a small fraction of the flare accelerated electrons escaped from the sun. Using their calculations, we find that for a similar power law electron energy spectrum and for typical streamer densities the total number of accelerated electrons in the corona with energies greater than 3 MeV for the 14 September, 1966 flare ranges from 4.5×10^{32} to 10^{34}. The values of N for this flare are quite consistent with those obtained above for the 7 July 1966 event. Since the observed electron fluxes at the earth for the 7 July 1966 and 14 September 1966 flares were comparable within an order of magnitude (Cline and McDonald, (1968), a comparison between the number of relativistic electrons accelerated in the flare and those trapped in the corona seems to imply that the high-energy electrons escape from the flare region into the corona relatively easily and without significant energy loss, but that escape from the corona into the interplanetary medium is seriously inhibited. Electrons with energies below mc^2, on the other hand, remain trapped in the microwave and x-ray emitting region where they rapidly lose their energy, mainly as a result of collisions, while at the same time they emit x-rays and microwaves by bremsstrahlung and gyro-synchrotron radiation.

Relatively easy escape for electrons above mc^2 from the x-ray and microwave producing region into the corona could conceivably lead to the high-energy cutoff in the spectrum of the radiating electrons which was required for the alternative model discussed above. It is not necessary, then, to associate this cutoff with the acceleration mechanism that produces the electrons. Both the

high-energy cutoff and the anisotropic models would be consistent with long-lived MeV electrons in the solar corona after the x-ray and microwave emissions have decayed away. These relativistic electrons, by being promptly released into a much larger volume that contains a much smaller magnetic field, would emit optically thin synchrotron radiation at lower frequencies and thus cause an upturn in the observed microwave spectrum at frequencies below about 10^3 MHz. Such "u" shaped bursts were observed on several occasions (Castelli, Aarons and Michael, 1967, 1968, Howard, 1968). The enhanced emission at decimeter wavelength, therefore, would correspond to synchrotron radiation from an optically thin source and thus an additional change in polarization would be expected at the transition from the optically thick microwave source to the optically thin decimeter emission. This seems also to be consistent with polarization measurements at decimeter wavelengths (Kai, 1965a).

In addition to comparing the deduced electron distribution to that observed at the earth at higher energies, we should, as well, seek to reconcile the model with the lower energy electrons in the region which produce soft x-rays. The soft x-ray component, in general, exhibits a rise time of several minutes (compared to the hard x-ray rise time of < 1 min), and a decay time of ~ 1 hr (Van Allen, 1967). Hudson, Peterson and Schwartz (1969) have found that all solar flare x-ray bursts above 8 keV, large and small, can be reconciled with a quasi-thermal emission measure of $\sim 10^{47}$ cm^{-3}, which remains constant during the

decay phase. If this emission measure was also characteristic of the region at the time of the hard x-ray maximum, we would be hard pressed to understand how as much as a few percent of the electrons in the volume could have energies in excess of 100 keV. The soft x-ray emission, however, does not achieve consistency with an emission measure of 10^{47} cm^{-3} until several minutes after soft x-ray maximum (which, in turn, may be as much as a few minutes after hard x-ray maximum). Neupert (1968) has found that, for one of the flares in the Hudson, Peterson and Schwartz (1969) sample, the emission measure at soft x-ray maximum is in excess of 10^{48} cm^{-3}, i.e. an order of magnitude greater a few minutes earlier in time. If this emission measure is more characteristic of the source region at x-ray maximum, then only a few tenths of a percent of the electrons in the volume have energies in excess of 100 keV.

We believe that the most reasonable model for the source region on a time scale of the order of several minutes is one in which the region is expanding. This would be consistent with a quasi-thermal emission measure which decreases in time, as well as with the observation that the microwave optical thickness also appears to decrease with time (i.e. type IV bursts occurring minutes after the primary bust have substantially larger flux densities at decimeter wavelengths than does the primary burst). The soft x-ray emission seems to arise from heating, possibly due to high-energy particle collision losses and plasma waves (approximately three orders of magnitude more energy is going into these modes than into x-ray and microwave emission from 100 keV electrons), which raise

the temperature of the source region to some tens of millions of degrees. The observations of the decay times of this emission of as long as $\sim$ 1 hr, coupled with the observation that the source region appears to reach a minimum emission measure of 10^{47} cm^{-3} which then remains constant throughout the decay, would indicate that the region mixes very little with the surrounding solar atmosphere.

SUMMARY

The hard x-ray (> 100 keV) and centimeter emission characterize the ignition of the flash phase of the large solar flare. The rise time of these emissions is of the order of seconds, reflecting the acceleration time of non-thermal electrons. These impulsively accelerated electrons have a generated spectrum which is well represented by a power law of the form $N(\gamma)\, d\gamma \propto (\gamma - 1)^{-(3-4)}$. We believe that a single source region of these non-thermal electrons is responsible for both emissions, since their temporal profiles are identical.

If there is no non-impulsive post-acceleration of the electrons, the constancy of the hard x-ray spectral shape throughout the decay phase indicates that collision is the prime energy loss mechanism. The ambient density of the medium must be $n \approx 10^{9-10}$ cm^{-3}, and the magnetic field probably cannot be larger than 400 gauss. The measured x-ray intensity, which is proportional to the non-thermal emission measure Nn, then determines the number of electrons with energy greater than the lower cutoff energy chosen for N. For the flare of 7 July 1966, Nn at maximum was $\sim 4.1 \times 10^{45}$ above 100 keV, so that $N_{max} \approx 4 \times 10^{35-36}$.

This number of electrons, with the deduced spectral shape, cannot reproduce the observed microwave radiation unless specific constraints are placed on the source medium and the electron distribution. It is found that at low microwave frequencies the radio source is optically thick as a result of reabsorption by the non-thermal electrons themselves. The transition from the optically thick to an optically thin regime at higher frequencies leads to a change in polarization at a frequency of about 3000 MHz, as was observed for the 7 July 1966 event. On the other hand, the Razin effect, gyro-resonance and free-free absorption have little effect on the radio spectrum at low frequencies. Consistent values of the parameters N/BA and α range from 10^{13} to 10^{15}, and 0.5 to 3, respectively, for the flare of 7 July 1966.

The radio emission at the high microwave frequencies (above ~10,000 MHz) must be suppressed by disabling the electrons with energies in excess of mc^2. This must be done by assuming either that the accelerated spectrum steepens considerably at energies $\gtrsim mc^2$, that the electrons have a highly anisotropic pitch-angle distribution, or that the high energy electrons can escape promptly from the source region into the corona. Such long-lived coronal MeV electrons would explain both the "U"-shaped bursts observed (and the additional charge in polarization which may occur at $\sim$ 1000 MHz), as well as the coronal type IV bursts sometimes observed hours after the flash phase. Although these relativistic electrons may escape from the source region easily, electron measurements at the earth would indicate that they are trapped in the solar corona, escaping into the interplanetary medium quite inefficiently.

The later development of the source region would seem to be characterized by an expansion of the source volume of an order of magnitude or more, during which time the development of the soft x-ray flare progresses. The source region appears to be fairly well insulated from the surrounding solar atmosphere, so that there is no apparent contradiction between the distinctly non-thermal hard x-ray burst on a time scale of a minute, and the more slowly cooling quasi-thermal x-ray emission from the region.

REFERENCES

1. Anderson, K. A., and Winckler, J. R.: 1962, J. Geophys. Res. 67, 4103.

2. Bekefi, G.: 1966, Radiation Processes in Plasmas, John Wiley & Sons, New York.

3. Berger, M. J., and Seltzer, S. M.: 1964, Tables of Energy Losses and Ranges of Electrons and Positrons, NASA SP-3012.

4. Boischot, A., and Clavelier, B.: 1967, Astrophys. Letters, 1, 7.

5. Castelli, J. P., Aarons, J., and Michael, G. A.: 1967, J. Geophys. Res. 72, 5491.

6. Castelli, J. P., Aarons, T., and Michael, G. A.: 1968, Astrophys. J. 153, 267.

7. Cline, T. L., Holt, S. S., and Hones, E. W.: 1968, J. Geophys. Res. 73, 434.

8. Cline, T. L. and McDonald, F. B.: 1968, Solar Physics, 5, 507.

9. DeJager, C.: 1967, Solar Physics 2, 327.

10. Elwert, G.: 1961, J. Geophys. Res. 66, 391.

11. Ginzburg, V. L.: 1964, The Propagation of Electromagnetic Waves in Plasmas, Pergamon Press, Oxford.

12. Hayakawa, S., and Kitao, K.: 1956, Prog. Theor. Phys. 16, 139.

13. Holt, S. S., and Cline, T. L.: 1968, Astrophys. J. 154, 1027.

14. Howard, E. G.: 1968, Ball Brothers Research Corp., Boulder, Colorado, TN68-33.

15. Hudson, H. S., Peterson, L. E., and Schwartz, D. A.: 1969, Astrophys. J. to be published.

16. Kai, K.: 1965a, Publ. Astron. Soc. Japan 17, 294.

17. Kai, K.: 1965b, Publ. Astron. Soc. Japan 17, 309.

18. Kakinuma, T., and Swarup, G.: 1962, Astrophys. J. 136, 975.

19. Kawabata, K.: 1964, Publ. Astron. Soc. Japan 16, 30.

20. Kundu, M. R.: 1961, J. Geophys. Res. 66, 4308.

21. Kundu, M. R.: 1965, Solar Radio Astronomy, Interscience, New York.

22. Liemohn, H. B.: 1965, Radio Sci. 69D, 741.

23. Nagoya University, Research Institute of Atmospherics, Toyokawa, Japan: 1966, Monthly Rept. of Solar Radio Emission, July 1966.

24. Neupert, W. M.: 1968, Astrophys. J. 153, L59.

25. Pawsey, J. L., and Bracewell, R. N.: 1955, Radio Astronomy, Clarendon Press, London.

26. Peterson, L. E., and Winckler, J. R.: 1959, J. Geophys. Res. 64, 697.

27. Ramaty, R.: 1968, J. Geophys. Res. 73, 3573.

28. Ramaty, R.: 1969, to be published.

29. Ramaty, R., and Lingenfelter, R. E.: 1967, J. Geophys. Res. 72, 879.

30. Ramaty, R., and Lingenfelter, R. E.: 1968, Solar Physics, to be published.

31. Takakura, T., and Kai, K.: 1966, Publ. Astron. Soc. Japan, 18, 57.

32. Twiss, R. Q.: 1958, Australian J. Phys. 11, 564.

33. Van Allen, J. A.: 1967, J. Geophys. Res. 72, 5903.

34. Zheleznyakov, V. V.: 1962, Soviet Astron. AJ 6, 3.

TABLE 1

Isotropic Electron Distribution with High-Energy Cutoff

$\frac{N}{BA}$	α	BN	B (gauss)	N(>100 kev)	n(cm^{-3})	α (calc)	$\bar{\alpha}$
10^{13}	1	2.5×10^{37}	260	$.96 \times 10^{35}$	4.3×10^{10}	0.58	0.7
	0.5	4.6×10^{37}	270	1.7×10^{35}	2.4×10^{10}	0.81	
	0.35	1.4×10^{38}	210	6.7×10^{35}	6.1×10^{9}	1.2	
10^{14}	1	7×10^{37}	170	4.1×10^{35}	10^{10}	0.8	0.8
	0.5	1.3×10^{38}	185	7×10^{35}	5.9×10^{9}	1.1	
	0.35	2.1×10^{38}	190	1.1×10^{36}	3.7×10^{9}	1.45	
10^{15}	1	2×10^{38}	105	1.9×10^{36}	2.2×10^{9}	1.05	$\gtrsim 1$
	0.5	2.5×10^{38}	110	2.3×10^{36}	1.8×10^{9}	1.2	
	0.35	3×10^{38}	112	2.7×10^{36}	1.5×10^{9}	1.35	

TABLE 2
Anisotropic Electron Distribution

$\frac{N}{BA}$	α	BN	B (gauss)	N(>100 kev)	n(cm^{-3})	α (calc)	$\overline{\alpha}$
10^{13}	1	7.6×10^{37}	350	2.3×10^{35}	1.8×10^{10}	1.2	$\gtrsim 1$
	0.5	2.8×10^{38}	370	7.5×10^{35}	5.5×10^{9}	1.9	
	0.35	–	–	–	–	–	
10^{14}	1	3.8×10^{38}	270	1.4×10^{36}	2.9×10^{9}	2.7	> 1
	0.5	6.2×10^{38}	280	2.2×10^{36}	1.9×10^{9}	3.0	
	0.35	–	–	–	–	–	
10^{15}	1	2×10^{39}	210	9.5×10^{36}	4.3×10^{8}	4.7	> 1
	0.5	3×10^{39}	220	1.3×10^{37}	3.2×10^{8}	5.7	
	0.35	7×10^{39}	240	2.9×10^{37}	1.4×10^{8}	9.5	

TABLE 3

$\frac{N}{BA}$	High Energy Cutoff					Anisotropic Pitch-Angle Distribution				
	$n(cm^{-3})$	B (gauss)	N(>100 kev)	$A(cm^2)$	$\bar{\gamma}$	$n(cm^{-3})$	B (gauss)	N(>100 kev)	$A(cm^2)$	$\bar{\gamma}$
10^{13}	3×10^{10}	265	1.4×10^{35}	4.9×10^{19}	2	2×10^{10}	350	2×10^{35}	5.7×10^{19}	1.6
10^{14}	8×10^{9}	180	5.1×10^{35}	2.3×10^{19}	2.7	3×10^{9}	270	1.3×10^{36}	4.8×10^{19}	1.8
10^{15}	2×10^{9}	100	2×10^{36}	2×10^{19}	3	5×10^{8}	210	8×10^{36}	3.8×10^{19}	1.94

FIGURE CAPTIONS

Figure 1. Microwave flux densities for a power law, normalized at the sun to 1 electron greater than 100 kev. The parameter α and N/BA are defined in Equations (19) and (22), respectively; the pitch-angle distributions corresponding to the isotropic and anisotropic cases are given in Equation 23; and the asterisks denote the frequency of polarization reversal.

Figure 2. Microwave flux densities for a power law with a high-energy cutoff, normalized at the sun to 1 electron greater than 100 kev. The parameters α and N/BA are defined in Equations (19) and (22), respectively; the pitch-angle distributions corresponding to the isotropic and anisotropic cases are given in Equation 23; and the asterisks denote the frequency of polarization reversal.

Figure 3. Differential electron spectrum as a function of time for various values of the ambient density n and magnetic field B; a choice of n determines all values of B and time (t) shown.

Figure 4. Time history of microwaves of 17000 MHz and x-rays greater than 80 kev for the flare of 7 July 1966 (after Cline, Holt and Hones (1968)).

Figure 5. Observed differential x-ray flux for the flare of 7 July 1966, together with the computed fluxes for two power law electron distributions.

The value of nN is 4.1×10^{45} for the spectral index -3, and 4×10^{46} for spectral index -5.

Figure 6. Observed microwave flux densities for the flare of 7 July 1966 together with computed microwave spectra for an isotropic distribution with a high-energy cutoff and an anisotropic distribution. The indicated values of B and n correspond to the values of the ambient field and density in a source region of constant density and uniform magnetic field.

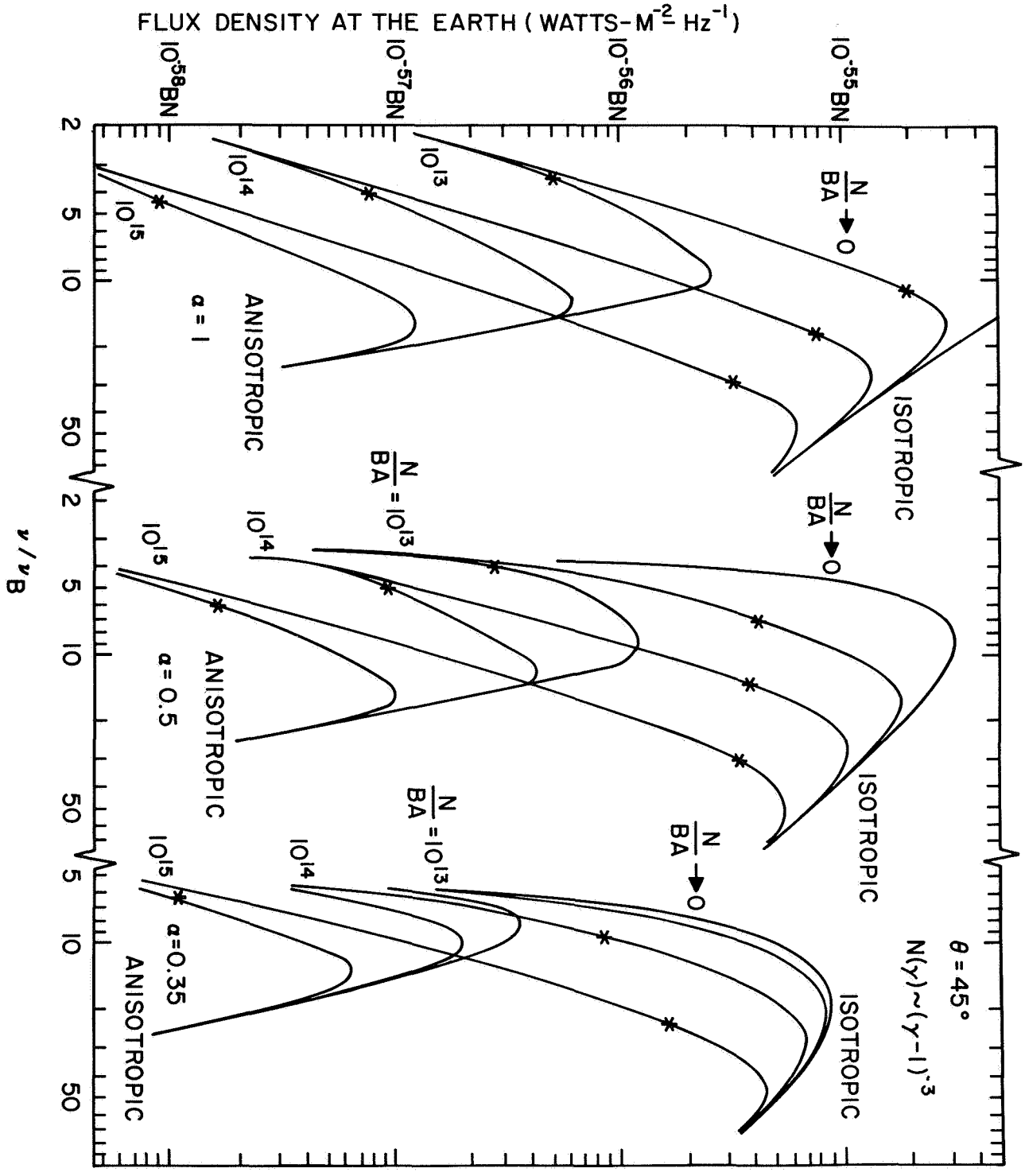
FLUX DENSITY AT THE EARTH (WATTS-M^{-2} Hz^{-1})
10^{-55}BN
10^{-56}BN
10^{-57}BN
10^{-58}BN
$\theta = 45°$
$N(\gamma) \sim (\gamma-1)^{-3}$
$\frac{N}{BA} \to 0$
ISOTROPIC
ANISOTROPIC
$\alpha = 1$
$\frac{N}{BA} = 10^{13}$
10^{13}
10^{14}
10^{15}
$\alpha = 0.5$
$\alpha = 0.35$
ν / ν_B
2
5
10
50

Figure 1

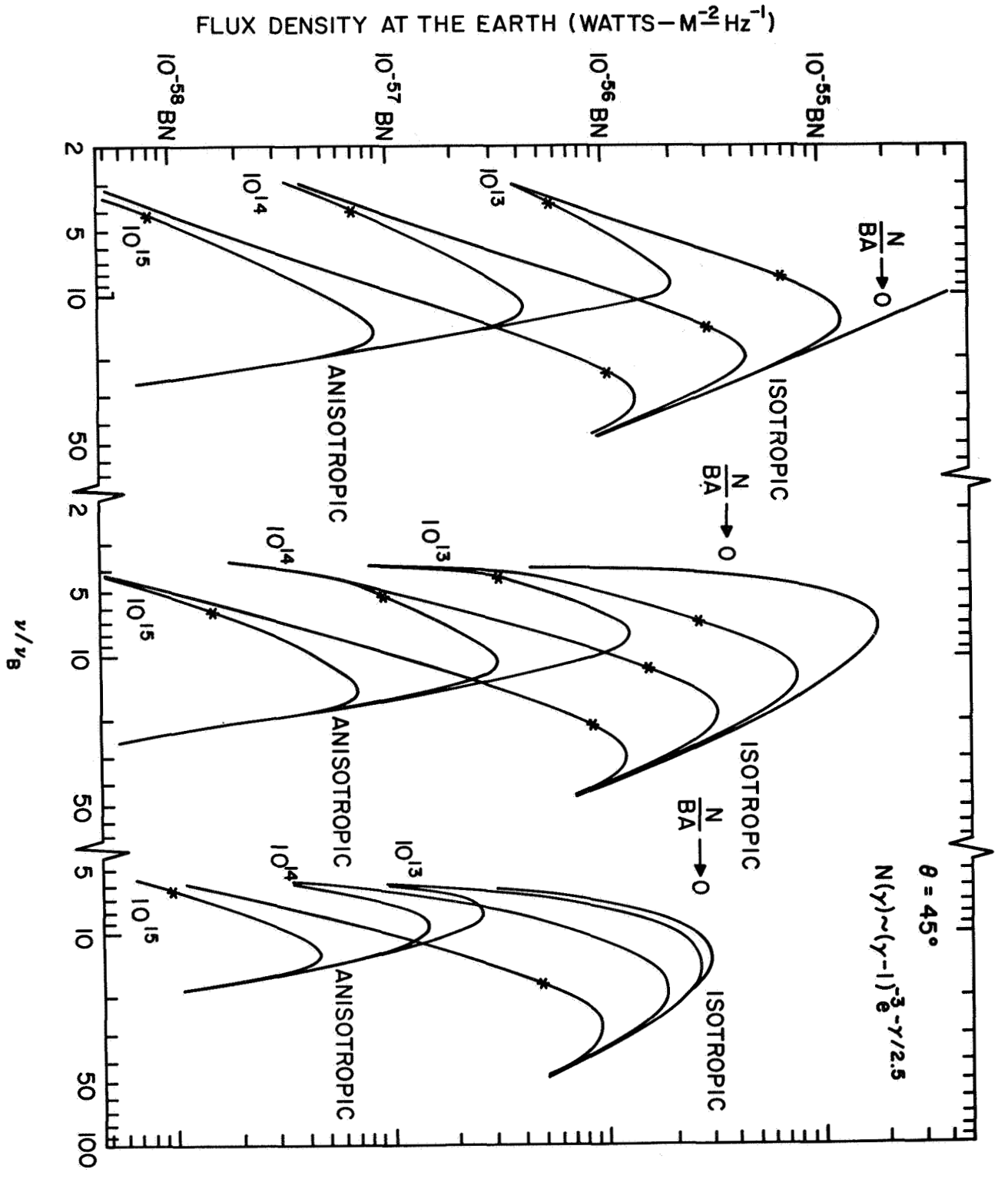
FLUX DENSITY AT THE EARTH (WATTS–M^{-2}Hz^{-1})
10^{-55}BN
10^{-56}BN
10^{-57}BN
10^{-58}BN
θ = 45°
N(γ)~(γ−1)$^{-3}$e$^{-\gamma/2.5}$
N/BA → 0
ISOTROPIC
ANISOTROPIC
10^{13}
10^{14}
10^{15}
2
5
10
50
100
ν/ν$_B$

Figure 2

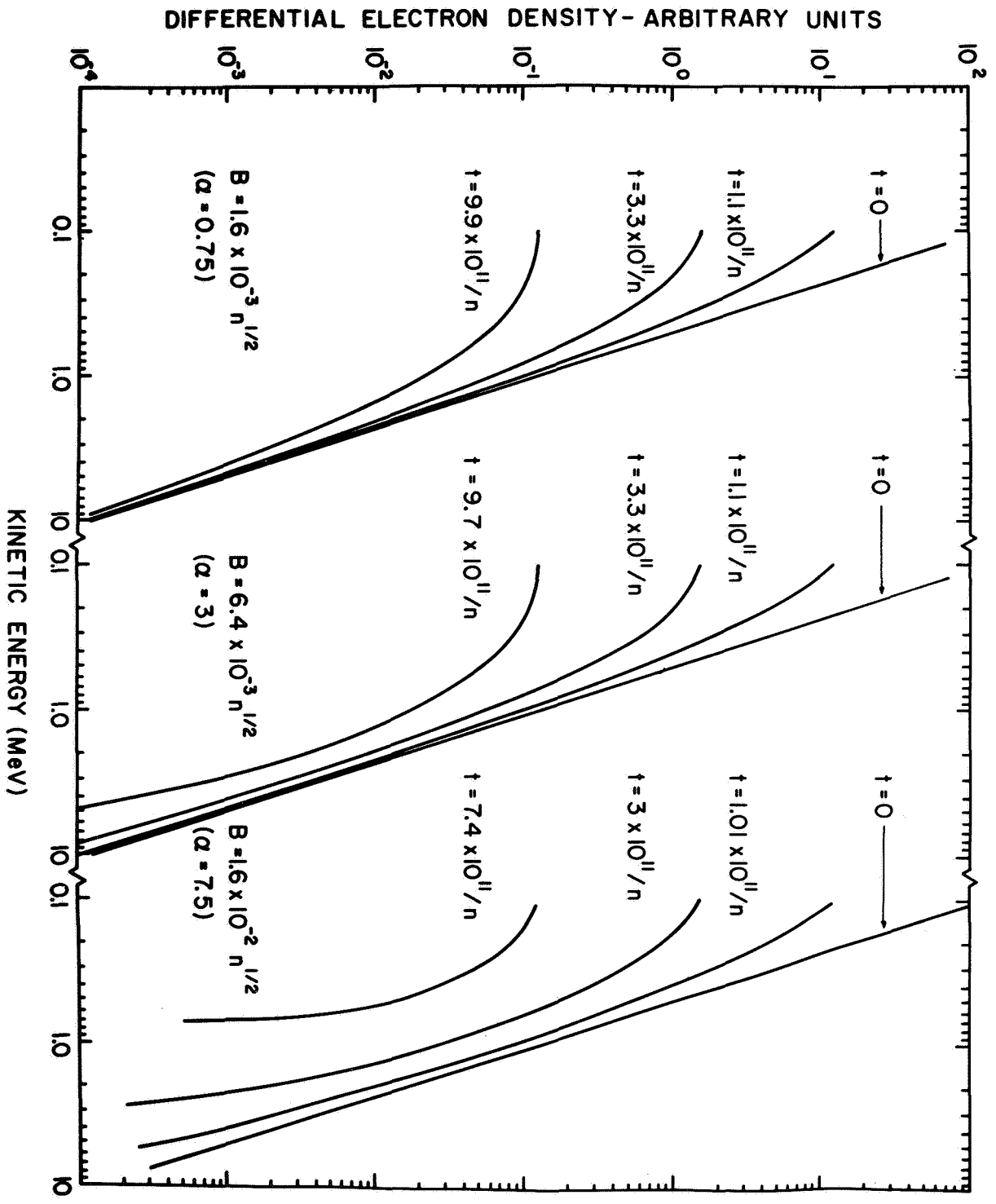
DIFFERENTIAL ELECTRON DENSITY - ARBITRARY UNITS
KINETIC ENERGY (MeV)
B = 1.6 x 10^-3 n^1/2 (α = 0.75)
t = 9.9 x 10^11/n
t = 3.3 x 10^11/n
t = 1.1 x 10^11/n
t = 0
B = 6.4 x 10^-3 n^1/2 (α = 3)
t = 9.7 x 10^11/n
t = 3.3 x 10^11/n
t = 1.1 x 10^11/n
t = 0
B = 1.6 x 10^-2 n^1/2 (α = 7.5)
t = 7.4 x 10^11/n
t = 3 x 10^11/n
t = 1.01 x 10^11/n
t = 0

Figure 3

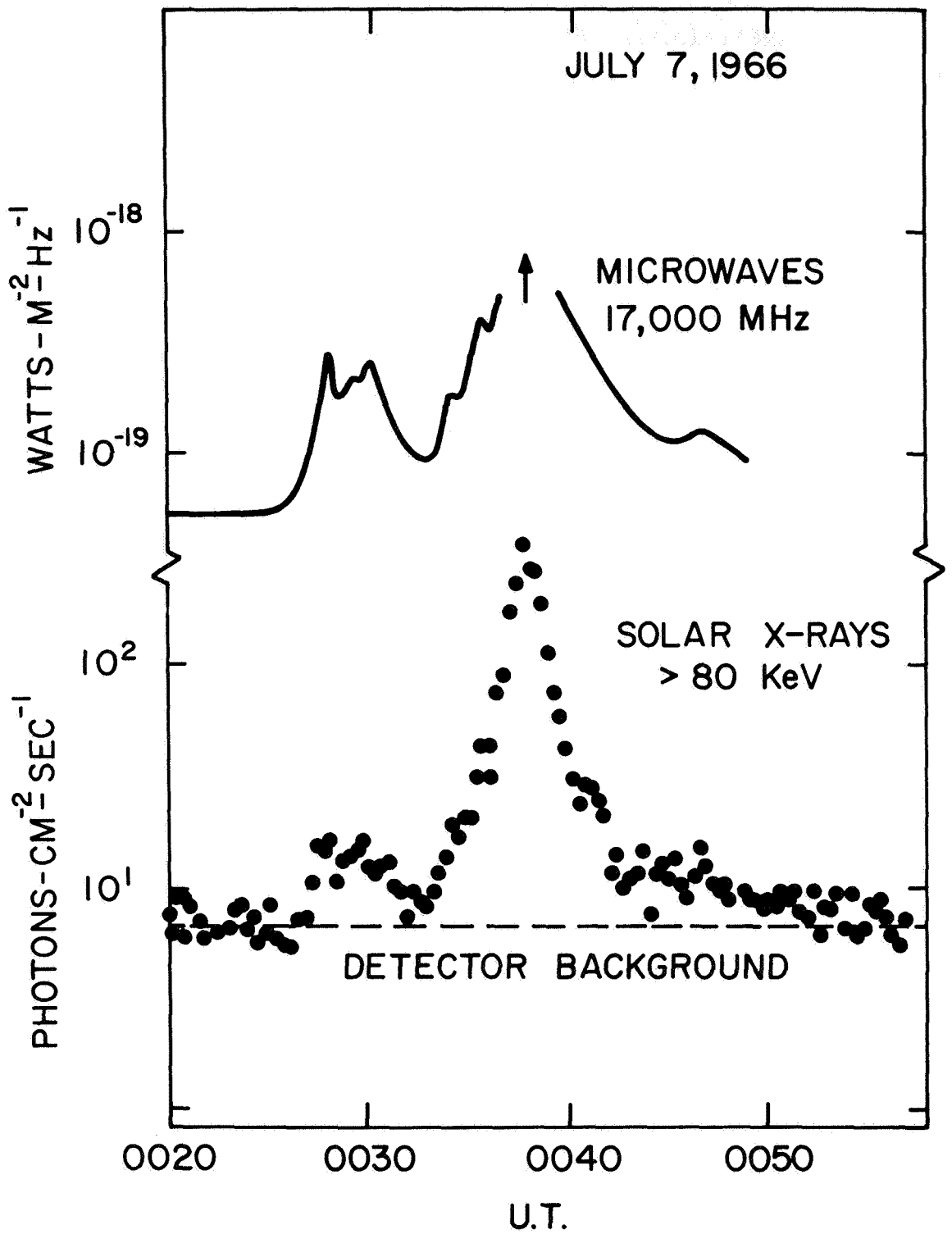
JULY 7, 1966
MICROWAVES
17,000 MHz
WATTS-M^{-2}-Hz^{-1}
10^{-18}
10^{-19}
SOLAR X-RAYS
> 80 KeV
PHOTONS-CM^{-2}-SEC^{-1}
10^{2}
10^{1}
DETECTOR BACKGROUND
0020
0030
0040
0050
U.T.

Figure 4

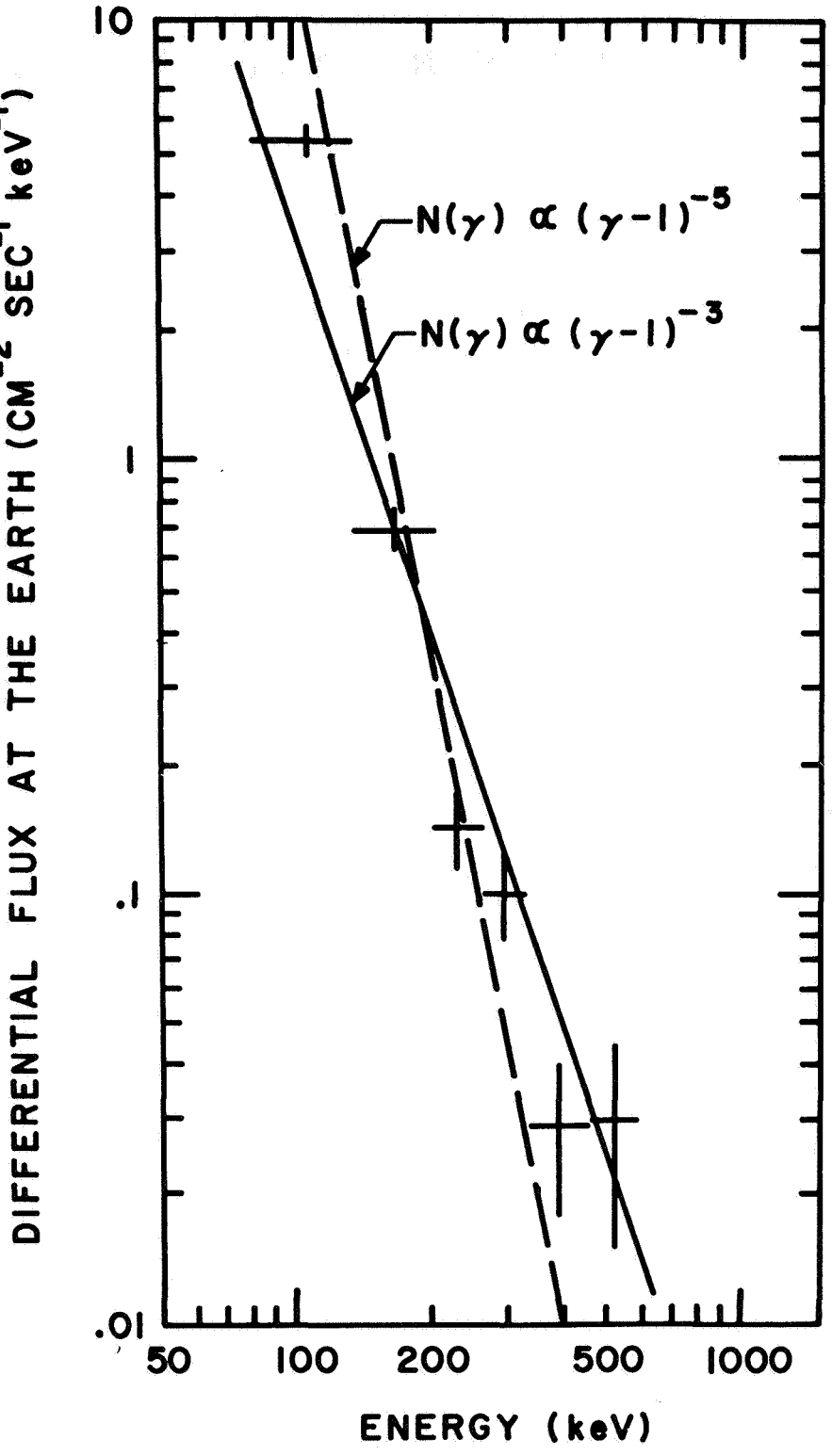
10
1
.1
.01
50
100
200
500
1000
ENERGY (keV)
DIFFERENTIAL FLUX AT THE EARTH (CM^{-2} SEC^{-1} keV^{-1})
N(γ) ∝ (γ-1)$^{-5}$
N(γ) ∝ (γ-1)$^{-3}$

Figure 5

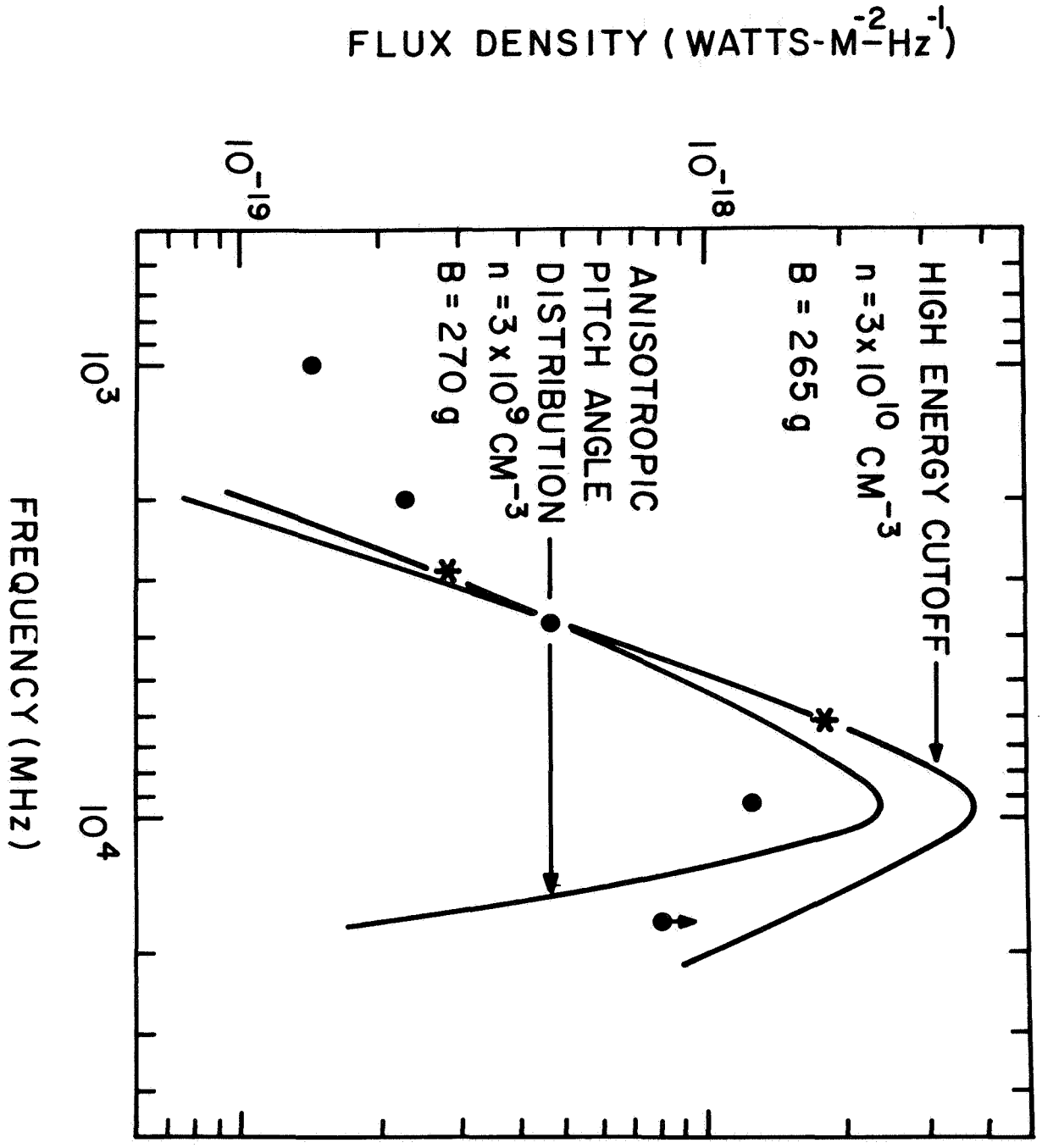
FLUX DENSITY (WATTS-M^{-2}Hz^{-1})
10^{-18}
10^{-19}
HIGH ENERGY CUTOFF
n = 3×10^{10} CM^{-3}
B = 265 g
ANISOTROPIC
PITCH ANGLE
DISTRIBUTION
n = 3×10^{9} CM^{-3}
B = 270 g
10^{3}
10^{4}
FREQUENCY (MHz)

Figure 6